EGG-PHYS-5654
DECEMBER 1981

COMPARISON OF COMPUTED REACTION RATES USING DIFFERENT METHODS AND DATA FOR THE STARFIRE AND TMHR BENCHMARK BLANKETS

A. J. Scott
M. L. Takata

U.S. Department of Energy
Idaho Operations Office • Idaho National Engineering Laboratory

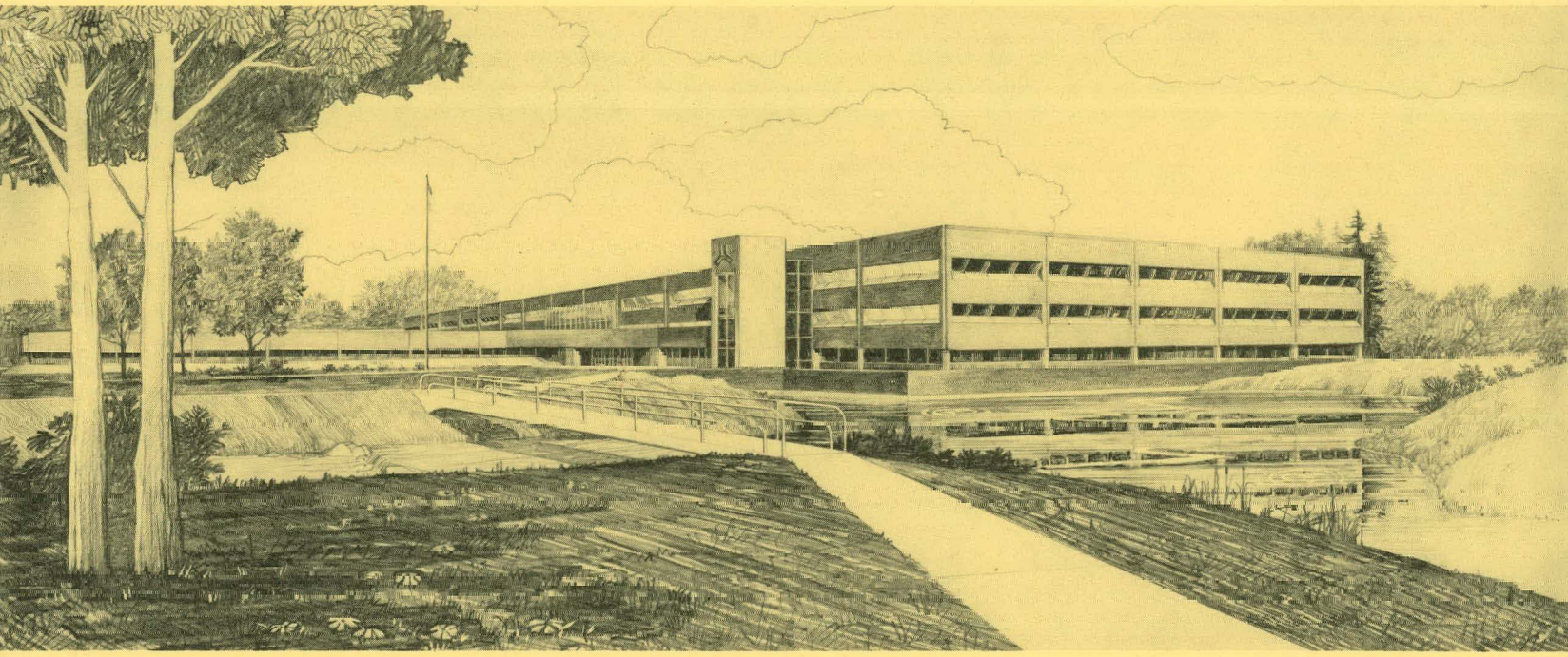

This is an informal report intended for use as a preliminary or working document

Prepared for the
U. S. Department of Energy
Idaho Operations Office
Under DOE Contract No. DE-AC07-76ID01570

EG&G Idaho

DISCLAIMER

EGG-PHYS--5654

DE82 010045

COMPARISON OF COMPUTED REACTION RATES USING DIFFERENT METHODS AND DATA FOR THE STARFIRE AND TMHR BENCHMARK BLANKETS

A. J. Scott
M. L. Takata

January 1982

EG&G Idaho, Inc.
Idaho Falls, Idaho 83415

Prepared for the
U. S. Department of Energy
Idaho Operations Office
Under DOE Contract No. DE-AC07-76ID01570

ABSTRACT

RAFFLE Monte Carlo calculations using ENDF/B V5 data have been performed for the TMHR suppressed fission benchmark blanket and the STARFIRE Reference Design blanket. One-dimensional cylindrical geometry was employed. ANISN S_N calculations were also done for both blankets using the DLC37F, FLUNG, and MACKLIB IV data sets. Reaction rates from RAFFLE and ANISN are compared with each other and with results obtained by the blanket designers (ANL, TRW, GA). The purposes of this study are to: 1) partially validate the new RAFFLE libraries for fusion neutronics and, 2) lend confidence to the results of previous ANISN calculations that were done to investigate the feasibility of fusion blanket testing in the Engineering Test Reactor. For both blankets, the tritium breeding ratio (TBR) predicted by RAFFLE and ANISN agree within 3%. For TMHR, our TBR results lie in between those obtained by TRW and GA, which disagree by 10-15%. For STARFIRE, our TBR results are 7-10% lower than ANL's values. The reason for the large discrepancies are unknown. However, it is concluded that modeling errors are unlikely so that data sources and processing differences used to generate cross section libraries are implied. Additional investigation is needed to resolve the differences.

CONTENTS

TABLES

TABLES (CONTINUED)

1. INTRODUCTION

The RAFFLE[1] Monte Carlo program has been used extensively at INEL to solve various neutron transport problems for fission reactors. However, until recently, it could not be applied to most fusion reactor problems because the cross section libraries contained data (processed from ENDF/B V4) only up to 10 MeV. This limitation has now been removed by a new cross section library derived from ENDF/B V5 data. RAFFLE and the ENDRAF[2] processing codes were both modified to treat high energy reactions (n,3n; n,p; etc.) and the new library energy range was extended to 16.9 MeV. To provide an initial test of the new library for fusion-neutron transport problems, reaction rates for two fusion reactor blankets were calculated with RAFFLE and compared to the results of ANISN[3] calculations. The blankets analyzed are the STARFIRE Reference Design blanket[4] and a neutronics benchmark blanket used in development of the suppressed fission Tandem Mirror Hybrid Reactor (TMHR)[5]. In addition to comparing with our own ANISN calculations, which used DLC37F[6], FLUNG[7], and MACKLIB IV[8] data libraries, the results are also compared with ANISN results computed by ANL (for STARFIRE) and GA (for TMHR). Also, for the TMHR benchmark blanket, results of TARTNP[9] Monte Carlo calculations done by TRW were available for comparison.

The intercomparison of results is intended not only as partial validation of the new RAFFLE libraries but also to validate the EG&G ANISN calculations that have been done in support of proposals[10,11] for fusion blanket testing in the Engineering Test Reactor (ETR). While the ANISN calculations for the ETR blanket testing employed methods and data that are widely used in the fusion community, comparison of the results for STARFIRE and the TMHR benchmark blanket with the results of the designers is intended to assure that data have been implemented and applied correctly. The report is divided into four parts. Details of the calculational methods along with a description of the blankets studied are given in Section 2. The results are compared and discussed in Section 3. Conclusions are presented in Section 4.

2.0 CALCULATIONAL METHODS & DATA

2.1 Blanket Descriptions

The STARFIRE Reference Design first wall/blanket system is fully described in Reference 4. For neutronics purposes, the region thicknesses and material compositions are given in Table 1 (reproduced from Reference 4). As shown in the table, STARFIRE carries two material options for the neutron multiplier region: beryllium or Zr_5Pb_3. We chose to analyze the beryllium multiplier. Atom densities for all materials, reproduced from Reference 4, are given in Table 2. With two exceptions, these densities were used. First, Table 2 lists densities for cold (room temperature) water. Since the inlet and outlet cooling water temperature is reported to be 280°C and 320°C respectively, atom densities for water at 300°C were used (Pressure = 15MPa). Second, SS-316 was substituted for the PCA steel in all regions. Atom densities for the hot water and SS-316 are given in Table 3. Use of SS-316 instead of PCA steel should have very little effect on tritium breeding rates. Finally, no attempt was made to represent the coolant header region, magnet shield, etc., that exist behind the reflector. Inclusion of these regions in detail would have made the calculations more expensive while having practically no effect on FW/Blanket reaction rates.

The TMHR benchmark blanket was devised by TMHR designers as a neutronics benchmark for TMHR blanket development. As such, it has been simplified to test neutronic methods and data and does not represent an actual blanket design envisioned for the TMHR. For example, the benchmark first wall is composed only of iron rather than a steel alloy, a more probable first wall candidate. (A discussion of TMHR blanket concepts is given in Reference 13.) Region thicknesses and material compositions for the TMHR benchmark provided by TRW and GA designers[12] are shown in Table 4. Material densities are given in Tables 5 and 6.

2.2 Calculational Models

The ANISN and RAFFLE calculations were done in cylindrical geometry with no axial leakage (i.e., cylinders are infinite in height). An S_8 angular quadrature and a P_3 scattering approximation were used in all ANISN calculations. The first wall radii were 2.14 m and 2 m for STARFIRE and TMHR, respectively. For STARFIRE, the fusion plasma source was assumed to emit neutrons isotropically and uniformly out to a radius of 1.5 m with an energy distribution given by:

$$f(E) = \exp\left[\frac{-5}{kT}\left(\sqrt{E}\right)^2 - \left(\sqrt{E_p}\right)^2\right]$$

where kT = 0.025 MeV and E_p = 14.07 MeV[14]. For TMHR, the source extended to 1.7 m and emitted neutrons only above 13.5 MeV to agree with the source description used by GA.

2.2.1 ANISN Cross Sections

The coupled 121-group (100n, 21g) DLC37F and 56-group (35n, 21g) FLUNG cross section sets were employed in the ANISN flux calculations. The DLC37F and FLUNG energy group structures are given in Tables 7 and 8 respectively.

Tritium production (i.e., the tritium breeding ratio) from ^{6}Li (n,α)T and ^{7}Li $(n,n'\alpha)$T reactions is computed from the ANISN multigroup flux solution as follows:

$$TBR = \sum_g \sum_r N\sigma_g \phi_{g,r}$$

where N is the atom density, σ_g is the group-dependent cross section and $\phi_{g,r}$ is the group and space-dependent flux normalized to one source neutron. Other reaction rates are computed in the same way. The cross section σ_g should obviously be consistent with the total cross section that was used in ANISN to compute the flux. The DLC37F library contains consistent tritium production cross sections as separate material data files. These were used in one case to compute the TBR. Two sets of data designated as "hot" and "cold" are present for ^{6}Li that differ only in the thermal group (#100).

In the "hot" set, the ^{6}Li cross sections were averaged over a 800K Maxwellian spectrum. The "cold" set was weighted with a 300K Maxwellian. The "hot" set was used in all ANISN calculations and in the auxiliary TBR computations.

The 171-group MACKLIB IV library was used in two cases to compute the TBR. When using fluxes generated with DLC37F, cross sections from MACKLIB IV were collapsed to the DLC37F 100-group energy structure with 1/E weighting. When using fluxes generated with FLUNG, the weighting functions used to collapse MACKLIB IV cross sections were taken from VITAMIN-C. The VITAMIN-C weighting functions are given in Table 9. These weighting schemes are consistent with the weighting used by ORNL to generate the DLC37F and FLUNG libraries. Since both the 171-group VITAMIN-C and MACKLIB IV libraries were also derived (from ENDF/B V4) using the Table 9 weighting, the collapsed 35-group FLUNG library and the collapsed TBR cross sections should be completely consistent[(a)]. Complete consistency is not obtained with DLC37F due to the fission and fusion neutron weighting spectra (Table 9) that were included in the original generation of MACKLIB IV but not in DLC37F. However, in the important energy range below 821 keV where almost all tritium production from ^{6}Li occurs, the DLC37F and collapsed TBR cross sections should be consistent. Retaining 100 groups in the calculations also reduces the effect of any inconsistencies in cross section weighting.

MACKLIB IV was not used to obtain thermal group tritium production. Instead, the ^{6}Li thermal group cross section (σ_g) was taken either from DLC37F or FLUNG, which use values of 507b and 750b respectively. The thermal-group cross section differences result from the different weighting spectra used. As mentioned above, the DLC37F value assumes an 800K Maxwellian while the FLUNG value assumes a 300K Maxwellian below 0.125 eV (Table 9). Since neither of these thermal cross sections are correct (i.e., the thermal neutron energy spectra will not be Maxwellian due to absorption hardening), the importance of the thermal cross sections used for STARFIRE tritium production was investigated. This is discussed in Appendix A. It is shown in

---

(a) Reference 8 reports the weighting used to generate MACKLIB IV data was "similar" to VITAMIN-C weighting.

Appendix A that the inappropriate weighting spectra assumed for DLC37F library generation causes a 1.3% overestimate of the STARFIRE TBR.

2.2.2 RAFFLE Cross Sections

Non-thermal (E> 0.414 eV) neutron cross sections used in RAFFLE were generated with the ENDRAF processing code from ENDF/B V5 files. Cross sections were weighted with an energy spectrum from Reference 15. In the thermal neutron energy range, ENDF/B V4 data were used for all isotopes except ^{232}Th. Version 5 data were used for thorium. The standard RAFFLE library group structure is shown in Table 10. Since RAFFLE treats non-elastic scattering events (n,2n; n,3n; inelastic scatter; etc.) through group transfer probability matrices, and since many high energy cross sections are changing rapidly with energy, a special library was also created with 34 groups above 10 MeV to eliminate uncertainties due to cross section weighting in ENDRAF. This multi-group energy structure is shown in Table 11. Due to a current 99-group limitation in RAFFLE, the group structure between 821 keV and 5 eV is more coarse (lethargy width = 0.5) than the standard library (lethargy width = 0.25) to accomodate the increased number of fast groups.

Pointwise resolved resonance cross sections were computed in RAFFLE during neutron tracking only for ^{232}Th. Room temperature was assumed in the Ψ, χ functions to Doppler-broaden the single-level Breit-Wigner cross-sections. The cross section contribution from the nearest eight neighboring resonances (four on each side) was considered to obtain the pointwise energy cross section. Resonance cross sections for thorium in the unresolved energy range were computed in RAFFLE by a probability table method similar to that reported in Reference 16. Resonance cross sections for iron, chromium, nickel, and manganese were precomputed by ENDRAF as infinite dilute.

3.0 RESULTS

3.1 STARFIRE Results

The total neutron absorption rates computed with ANISN and RAFFLE for each region of the STARFIRE first wall/blanket system are compared in Table 12. The RAFFLE results agree with each other within the statistical uncertainties. Agreement with ANISN results are reasonably good considering the different methods and data sources used. The total neutron loss is in good agreement which implies that the neutron multiplication from n,2n reactions is also in good agreement. The difference in the two ANISN absorption rates for the first and second wall regions is mainly due to the much higher thermal-group absorption cross sections for steel in the FLUNG library than those in the DLC37F library. As mentioned in Section 2, this results from differences in the thermal-neutron energy spectrum that was assumed for a weighting function to compute the single thermal-group cross sections from the pointwise (energy-dependent) cross section data. RAFFLE employs 22 groups below 0.414 eV so that cross section weighting in the thermal range is relatively unimportant.

The ANISN (EG&G) and RAFFLE tritium breeding ratio (TBR) for the blanket are compared with the published ANL results in Table 13. A serious discrepancy is seen between the ^{6}Li TBR obtained by ANL and all of the EG&G results. The fact that all our results, which were obtained from different cross section libraries and codes, agree reasonably well with each other but disagree with ANL's results suggests a modeling difference between our model and that used by ANL. A check with ANL uncovered several minor modeling differences that were individually evaluated for their effect on the TBR[17].

First, ANL used an S_4 angular quadrature in ANISN while we used S_8. The effect of the more coarse angular quadrature was found from 100-group ANISN calculations to overestimate the TBR by 1%. This would explain part of the discrepancy. Another model difference was in the water density assumed. Since the blanket inlet and outlet coolant densities were reported in Reference 4 as 280°C and 320°C (15 MPa) respectively, we used 300°C water. This water temperature was also assumed for the first wall, second wall, and reflector. ANL used cold (room temperature) water. The effect of using cold

water densities was determined with a 35-group (FLUNG library) ANISN calculation. Compared to the results in Table 13, the cold water reduced the TBR by 1% due to increased moderation and parasitic capture in the walls and multiplier region. This difference compensates for the angular quadrature effect. A third model difference existed in the fusion-neutron source energy distribution. We assumed the plasma source to emit neutrons in the exponential distribution given in Reference 14 (see Section 2). Integrating this function results in about 94% of the neutron source occurring in Group 1 (DLC37 or FLUNG group structure) and 6% in Group 2. ANL assumed all neutrons to be emitted in Group 1. A 35-group (FLUNG) ANISN calculation was made with the ANL source representation. The blanket TBR was increased by about 0.4% with the higher energy source due to increased penetration of the first wall, multiplier, and second wall regions thus allowing more neutrons to reach the blanket.

A final modeling difference concerns a small amount of beryllium coating on the first wall that was omitted in our calculations but included in ANL's model. Reference 4 reports the beryllium layer to be 1 mm thick. ANL designers stated the layer to be a "few" millimeters thick. ANISN calculations with FLUNG resulted in a TBR increase of 1.3% with 2mm of beryllium on the first wall.

The net effect of all the small differences in our ANISN model and ANL's ANISN model would be to improve the TBR agreement by about 1.7%. A significant discrepancy still remains.

3.2 TMHR Results

Table 14 compares various reaction rates computed in this study for the TMHR benchmark with TARTNP and ANISN results obtained by TRW and GA, respectively. All our results for tritium production from ^{6}Li agree quite well with each other and lie in between the TARTNP and ANISN(GA) results. In the case of ^{7}Li, all results are in good agreement except TARTNP. TARTNP results are 6% or more lower than the results of the other codes.

4.0 CONCLUSIONS

The intent of this study was to partially validate the new RAFFLE libraries for fusion applications and the results of ANISN calculations that were done in support of fusion blanket testing in ETR. For the TMHR benchmark, our tritium breeding results lie in between those of TRW and GA. Other reaction rates are generally higher than TRW's results and in fair agreement with GA's results. Our tritium breeding results for STARFIRE are significantly lower than ANL's results. Validation has been achieved only to the extent that our results are "in the ballpark".

The discrepancies are probably not due to modeling errors (geometry, material compositions, etc.) since the blanket problems are so simple. This implies then, that cross section data or data processing are probably responsible. For example, both the FLUNG library and one of the libraries used by GA were collapsed from VITAMIN-C, yet the ^{6}Li TBR disagrees by 15%. This could be due to the weighting functions used in collapsing, or to the fact that GA used the older MACKLIB data to compute the TBR whereas we used MACKLIB IV. (MACKLIB was not available for cross section comparison.) Again, RAFFLE and TARTNP calculations both used ENDFB/V5 data but the two Monte Carlo codes predict a ^{6}Li tritium breeding that differs by 7%. A likely candidate for this discrepancy is the processing and treatment of the Be(n,2n) data. This conclusion is based on the dual observation that: 1) RAFFLE predicts most reaction rates to be 6% or more higher than TARTNP values which implies that general flux levels are higher by 6% or more, and, 2) the total neutron source after multiplication by n,2n reactions (most of which is Be) is 2.6 in RAFFLE compared to 2.4 in TARTNP. If the Be(n,2n) reaction rate agreed, then the total source would agree and all reaction rates except Fe(n,p) and Fe(n,α) would then be in good agreement. A review and further testing of the cross section data processing are needed.

The obvious problem with an intercomparison of results from different methods and data for validation purposes is that the "true" answers are not known. Since the discrepancies in important parameters like tritium breeding and beryllium neutron multiplication are so large, analyses of some good, well-defined experiments would be useful. This possibility will be investigated.

5.0 REFERENCES

1. F. J. Wheeler, et. al., The RAFFLE V General Purpose Monte Carlo Code for Neutron and Gamma Transport, to be published.

2. R. A. Grimesey, private communication, EG&G Idaho, Inc., July 1981.

3. W. W. Engle, Jr., A User's Manual for ANISN, A One-Dimensional Discrete Ordinates Transport Code with Anisotropic Scattering, K-1693, Computing Technology Center, 1967.

4. STARFIRE - A Commercial Tokamak Fusion Power Plant Study, Argonne National Laboratory Report, ANL/FPP-80-1, September 1980.

5. D. H. Berwald (TRW) to G. R. Imel (EG&G), private communication, March 12, 1981.

6. D. M. Plaster, R. T. Santoro, W. E. Ford, III, Coupled 100-Group Neutron and 21-Group Gamma-Ray Cross Sections for EPR Calculations, DLC-37, ORNL-TM-4812, April 1975, updated to DLC-37F, October 1979.

7. R. T. Santoro, R. W. Roussin, J. M. Barnes, FLUNG: Coupled 35-Group Neutron and 21-Group Gamma Ray, P_3 Cross Sections for Fusion Applications, ORNL/TM-7828, June 1981.

8. Y. Gohar and M. A. Abdou, MACKLIB-IV A Library of Nuclear Response Functions Generated with the MACK-IV Computer Program from ENDF/B-IV, ANL/FPP/TM-106, March 1978.

9. J. Kimlinger and E. Plechaty, TARTNP Users Manual, UCID-17026, Lawrence Livermore National Laboratory, 1976.

10. P. Y. S. Hsu, G. R. Longhurst, and L. G. Miller, "Concepts for Testing Fusion First Wall/Blanket Systems in Existing Nuclear Facilities", Fourth Topical Meeting on the Technology of Controlled Nuclear Fusion, King of Prussia, PA., October 1980.

11. D. E. Wessol, et. al., Physics Calculations for Preliminary Studies of Fusion Blanket Testing in ETR, EG&G-PHYS-5392, EG&G Idaho, Inc., March 1981.

12. E. Cheng (GA) to G. R. Imel (EG&G), private communication, March 1981.

13. J. A. Maniscalco, et. al., "Recent Progress in Fission-Fusion Hybrid Reactor Design Studies", Nuclear Technology/Fusion, Vol. 1, pp. 419, October 1981.

14 R. W. Roussin, et. al, VITAMIN-C: The CTR Processed Multigroup Cross Section Library for Neutronics Studies, ORNL/RSIC-37, 1980; also available as DLC-41.

15. W. B. Wilson, et.al., Multigroup and Few-Group Cross Sections for ENDF/B-IV Fission-Products; the TOAFEW Collapsing Code and Data File of 154-Group Fission-Product Cross Sections, LA-7174-MS (Informal Report), NRC-1, March 1978.

16. D. E. Cullen, et. al., "Cross Section Probability Tables in Multigroup Transport Calculations", A Review of Multigroup Nuclear Cross-section Processing Proceedings of a Seminar-Workshop, Oak Ridge, TE, ORNL/RSIC-41, March 1978.

17. Y. Gohar, private communication, EG&G, Idaho Inc., October 1981.

TABLE 1. BLANKET PARAMETERS FOR STARFIRE REFERENCE DESIGN

Zone Description	Zone Description (cm)	Zone Composition Percentage by Volume
First Wall	1	50% PCA steel structure 27% H_2O coolant
Neutron Multiplier	5	100% Zr_5Pb_3 or 70% Be
Second Wall	1	35% PCA steel structure 17% H_2O coolant
Tritium Breeder	30	80% $LiAlO_2$ tritium breeding material[a] 10% PCA steel structure 5% H_2O coolant 5% He purge stream
Reflector	15	90% carbon reflector 5% PCA steel structure 5% H_2O coolant

[a] Natural Li for Be neutron multiplier or enriched 60% ^6Li for the Zr_5Pb_3 neutron multiplier.

TABLE 2. DENSITIES OF CANDIDATE NEUTRON MULTIPLIER MATERIALS FOR STARFIRE

Material	Density (gm/cm^3)	Density ($atom/cm^3 \times 10^{24}$)	
Li_2O*	2.023	O	0.04078
		Li	0.08156
Li_7Pb_2	4.59	Pb	0.01194
		Li	0.04180
$LiAlO_2$	3.40	O	0.06211
		Al	0.03106
		Li	0.03106
Li_2SiO_3	2.52	O	0.05061
		Si	0.01687
		Li	0.03374
Be	1.85	Be	0.1236
BeO	2.96	Be	0.07127
		O	0.07127
Zr	6.5	Zr	0.04291
Pb	11.34	Pb	0.03348
PbO	9.53	Pb	0.02571
		O	0.02571
Zr_5Pb_3	8.93	Zr	0.02340
		Pb	0.01400
H_2O	1.0	H	0.0670
		O	0.0335
D_2O	1.1	D	0.0664
		O	0.0332
Ferritic Steel	7.7	C	0.0003089
		V	0.0001365
		Cr	0.008027
		Fe	0.07404
		Nb	0.00004991
		Mo	0.0004834
		W	0.0001261

* A density factor of 0.6 is used with Li_2O in all the neutronic analysis.

TABLE 2. (Continued)

Material	Density (gm/cm^3)	Density ($atom/cm^3 \times 10^{24}$)	
PCA Steel	7.81	Fe	0.05486
		Cr	0.01266
		Ni	0.01282
		Mo	0.0009793
		Mn	0.001710
		Ti	0.0002942
		Si	0.0008384
		C	0.0001961
		N	0.00003358
C	1.6	C	0.08023

TABLE 3. ATOM DENSITIES FOR HOT WATER AND SS-316

Material	Isotope	Density ($atoms/cm^3 \times 10^{24}$)
Water (300°C, 15 MPa)	H	0.0486
	O	0.0243
SS-316	Fe	0.05657
	Ni	0.00988
	Cr	0.01581
	Mn	0.00176
	Mo	0.00126
	Si	0.00172
	C	0.00032
	P	0.00007
	S	0.00005

TABLE 4. TMHR BENCHMARK DESCRIPTION

Zone	Width(cm)	Composition
1	200.0	Plasma (Void)
2	0.5	100% Fe
3	10.0	5% Fe 94% Be 1% LiO_2
4	20.0	5% Fe 93% Be 2% Th
5	30.0	100% C

TABLE 5. ATOM DENSITIES OF THE PURE MATERIALS IN TMHR

	Density (g/cm^3)	Atomic Weight	Density ($atoms/cm^3 \times 10^{24}$)
Be	1.85	9.012	1.23641×10^{-1}
Fe	7.86	55.85	8.47641×10^{-2}
^{232}Th	11.70	232.40	3.03694×10^{-2}
C	1.60	12.01	8.02400×10^{-2}
Li_2O*	2.035	29.8835	
^{6}Li		6.015	6.08440×10^{-3}
^{7}Li		7.016	7.59156×10^{-2}
O		16.00	4.10000×10^{-2}

* Natural lithium, 7.42 at% Li-6.

TABLE 6. VOLUME-WEIGHTED ATOM DENSITIES IN THE TMHR BLANKET

Region	Composition	Isotope	Density (atoms/cm^3 x 10^{24})
First Wall	100% Fe	Fe	8.47641×10^{-2}
Tritium Breeder	5% Fe,	Fe	4.32821×10^{-3}
	94% Be,	Be	1.16223×10^{-1}
	1% Li_2O	Li-6	6.08440×10^{-5}
		Li-7	7.59156×10^{-4}
		O	4.10000×10^{-4}
U-232 Breeder	5% Fe,	Fe	4.23821×10^{-3}
	93% Be,	Be	1.14986×10^{-1}
	2% Th	Th	6.07388×10^{-4}
Reflector	100% C	C	8.02400×10^{-2}

TABLE 7. DLC 37 100-GROUP ENERGY STRUCTURE

Group	Energy Range (eV)		Group	Energy Range (eV)	
1	1.4915E 07*	1.3499E 07	51	8.6517E 04	6.7380E 04
2	1.3499E 07	1.2214E 07	52	6.7380E 04	5.2475E 04
3	1.2214E 07	1.1052E 07	53	5.2475E 04	4.0868E 04
4	1.1052E 07	1.0000E 07	54	4.0868E 04	3.1828E 04
5	1.0000E 07	9.0484E 06	55	3.1828E 04	2.4788E 04
6	9.0484E 06	8.1873E 06	56	2.4788E 04	1.9305E 04
7	8.1873E 06	7.4082E 06	57	1.9305E 04	1.5034E 04
8	7.4082E 06	6.7032E 06	58	1.5034E 04	1.1709E 04
9	6.7032E 06	6.0653E 06	59	1.1709E 04	9.1188E 03
10	6.0653E 06	5.4881E 06	60	9.1188E 03	7.1018E 03
11	5.4881E 06	4.9659E 06	61	7.1018E 03	5.5309E 03
12	4.9659E 06	4.4933E 06	62	5.5309E 03	4.3074E 03
13	4.4933E 06	4.0657E 06	63	4.3074E 03	3.3546E 03
14	4.0657E 06	3.6788E 06	64	3.3546E 03	2.6126E 03
15	3.6788E 06	3.3287E 06	65	2.6126E 03	2.0347E 03
16	3.3287E 06	3.0119E 06	66	2.0347E 03	1.5846E 03
17	3.0119E 06	2.7253E 06	67	1.5846E 03	1.2341E 03
18	2.7253E 06	2.4660E 06	68	1.2341E 03	9.6112E 02
19	2.4660E 06	2.2313E 06	69	9.6112E 02	7.4852E 02
20	2.2313E 06	2.0190E 06	70	7.4852E 02	5.8295E 02
21	2.0190E 06	1.8268E 06	71	5.8295E 02	4.5400E 02
22	1.8268E 06	1.6530E 06	72	4.5400E 02	3.5358E 02
23	1.6530E 06	1.4957E 06	73	3.5358E 02	2.7537E 02
24	1.4957E 06	1.3534E 06	74	2.7537E 02	2.1445E 02
25	1.3534E 06	1.2246E 06	75	2.1445E 02	1.6702E 02
26	1.2246E 06	1.1080E 06	76	1.6702E 02	1.3007E 02
27	1.1080E 06	1.0026E 06	77	1.3007E 02	1.0130E 02
28	1.0026E 06	9.0718E 05	78	1.0130E 02	7.8893E 01
29	9.0718E 05	8.2085E 05	79	7.8893E 01	6.1442E 01
30	8.2085E 05	7.4274E 05	80	6.1442E 01	4.7851E 01
31	7.4274E 05	6.7206E 05	81	4.7851E 01	3.7267E 01
32	6.7206E 05	6.0810E 05	82	3.7267E 01	2.9023E 01
33	6.0810E 05	5.5023E 05	83	2.9023E 01	2.2603E 01
34	5.5023E 05	4.9787E 05	84	2.2603E 01	1.7604E 01
35	4.9787E 05	4.5049E 05	85	1.7604E 01	1.3710E 01
36	4.5049E 05	4.0762E 05	86	1.3710E 01	1.0677E 01
37	4.0762E 05	3.6883E 05	87	1.0677E 01	8.3153E 00
38	3.6883E 05	3.3373E 05	88	8.3153E 00	6.4760E 00
39	3.3373E 05	3.0197E 05	89	6.4760E 00	5.0435E 00
40	3.0197E 05	2.7324E 05	90	5.0435E 00	3.9279E 00
41	2.7324E 05	2.4724E 05	91	3.9279E 00	3.0590E 00
42	2.4724E 05	2.2371E 05	92	3.0590E 00	2.3824E 00
43	2.2371E 05	2.0242E 05	93	2.3824E 00	1.8554E 00
44	2.0242E 05	1.8316E 05	94	1.8554E 00	1.4450E 00
45	1.8316E 05	1.6573E 05	95	1.4450E 00	1.1254E 00
46	1.6473E 05	1.4996E 05	96	1.1254E 00	8.7644E-01
47	1.4996E 05	1.3569E 05	97	8.7644E-01	6.8257E-01
48	1.3569E 05	1.2277E 05	98	6.8257E-01	5.3159E-01
49	1.2277E 05	1.1109E 05	99	5.3159E-01	4.1400E-01
50	1.1109E 05	8.6517E 04	100	4.1400E-01	1.0000E-04

*Read 1.4918×10^7.

TABLE 8. FLUNG 35-GROUP ENERGY STRUCTURE

Group	Neutron Lower Energy (eV)	Group	Neutron Lower Energy (eV)
1	1.3499(07)*	19	2.2371(05)
2	1.2214(07)	20	1.4996(05)
3	1.0000(07)	21	8.6517(04)
4	8.1873(06)	22	3.1828(04)
5	6.7032(06)	23	1.5034(04)
6	5.4881(06)	24	7.1018(03)
7	4.4933(06)	25	3.3546(03)
8	3.6788(06)	26	1.5846(03)
9	3.0119(06)	27	4.5400(02)
10	2.4660(06)	28	1.0130(02)
11	2.0190(06)	29	2.2603(01)
12	1.6530(06)	30	1.0677(01)
13	1.3534(06)	31	5.0435(00)
14	1.1080(06)	32	2.3824(00)
15	9.0718(05)	33	1.1254(00)
16	7.4274(05)	34	4.1400(-01)
17	4.9787(05)	35	1.0000(-05)
18	3.3373(05)		

*Upper energy for neutron group 1 is 1.4918(07).

Table 9. Neutron Energy Weighting Function

Functional Form	Energy Limits
(1) Maxwellian Thermal Spectrum (300 K) $S_1(E) = C_1 E e^{-E/kT}$	10^{-5} eV to 0.125 eV
(2) "1/E" Slowing-Down Spectrum $S_2(E) = C_2/E$	0.125 eV to 820.8 keV
(3) Fission Spectrum (Θ = 1.4 MeV) $S_3(E) = C_3 E^{1/2} e^{-E/\Theta}$	820.8 keV to 10.0 MeV
(4) "1/E" Spectrum $S_4(E) = C_4/E$	10.0 MeV to 12.57 MeV
(5) Velocity Exponential Fusion Peak (E_p = 14.07 MeV) (kT = 0.025 MeV) $S_5(E) = C_5 \exp\left\{-\frac{5}{kT}\left(E^{1/2} - E_p^{1/2}\right)^2\right\}$	12.57 MeV to 15.57 MeV
(6) "1/E" Spectrum $S_6(E) = C_6/E$	15.57 MeV to 17.333 MeV

TABLE 10. RAFFLE 94-GROUP ENERGY STRUCTURE

GROUP	GROUPSET	LOWER ENERGY(EV)	GROUP	GROUPSET	LOWER ENERGY(EV)
1	1	1.4918E+07	48	48	1.6702E+02
2	2	1.3499E+07	49	49	1.3007E+02
3	3	1.1912E+07	50	50	1.0130E+02
4	4	1.0000E+07	51	51	7.8893E+01
5	5	7.7880E+06	52	52	6.1442E+01
6	6	6.0653E+06	53	53	4.7851E+01
7	7	4.7237E+06	54	54	3.7267E+01
8	8	3.6788E+06	55	55	2.9023E+01
9	9	2.8650E+06	56	56	2.2603E+01
10	10	2.2313E+06	57	57	1.7603E+01
11	11	1.7377E+06	58	58	1.3710E+01
12	12	1.3534E+06	59	59	1.0677E+01
13	13	1.0540E+06	60	60	8.3153E+00
14	14	8.2085E+05	61	61	6.4760E+00
15	15	6.3928E+05	62	62	5.0435E+00
16	16	4.9787E+05	63	63	3.9279E+00
17	17	3.8774E+05	64	64	3.0590E+00
18	18	3.0197E+05	65	65	2.3824E+00
19	19	2.3518E+05	66	66	1.8554E+00
20	20	1.8316E+05	67	67	1.4450E+00
21	21	1.4264E+05	68	68	1.1254E+00
22	22	1.1109E+05	69	69	8.7642E-01
23	23	8.6517E+04	70	70	6.8256E-01
24	24	6.7379E+04	71	71	5.3158E-01
25	25	5.2475E+04	72	72	4.1399E-01
26	26	4.0868E+04	73	73	3.8000E-01
27	27	3.1828E+04	74	74	3.6000E-01
28	28	2.4788E+04	75	75	3.3000E-01
29	29	1.9305E+04	76	76	3.1000E-01
30	30	1.5034E+04	77	77	3.0000E-01
31	31	1.1709E+04	78	78	2.9000E-01
32	32	9.1188E+03	79	79	2.8000E-01
33	33	7.1017E+03	80	80	2.6000E-01
34	34	5.5308E+03	81	81	2.4000E-01
35	35	4.3074E+03	82	82	2.2000E-01
36	36	3.3546E+03	83	83	1.8000E-01
37	37	2.6126E+03	84	84	1.6000E-01
38	38	2.0347E+03	85	85	1.4000E-01
39	39	1.5846E+03	86	86	1.0000E-01
40	40	1.2341E+03	87	87	8.0000E-02
41	41	9.6112E+02	88	88	6.0000E-02
42	42	7.4852E+02	89	89	4.0000E-02
43	43	5.8295E+02	90	90	2.5300E-02
44	44	4.5400E+02	91	91	1.5000E-02
45	45	3.5358E+02	92	92	7.0000E-03
46	46	2.7536E+02	93	93	4.0000E-03
47	47	2.1445E+02	94	94	0.

TABLE 11. RAFFLE 99-GROUP ENERGY STRUCTURE

GROUP	GROUPSET	LOWER ENERGY(EV)	GROUP	GROUPSET	LOWER ENERGY(EV)
1	1	1.6000E+07	50	50	4.0868E+04
2	2	1.5500E+07	51	51	2.4788E+04
3	3	1.5375E+07	52	52	1.5034E+04
4	4	1.5250E+07	53	53	9.1188E+03
5	5	1.5125E+07	54	54	5.5308E+03
6	6	1.5000E+07	55	55	3.3546E+03
7	7	1.4875E+07	56	56	2.0347E+03
8	8	1.4750E+07	57	57	1.2341E+03
9	9	1.4625E+07	58	58	7.4852E+02
10	10	1.4500E+07	59	59	4.5400E+02
11	11	1.4375E+07	60	60	2.7536E+02
12	12	1.4250E+07	61	61	1.6702E+02
13	13	1.4125E+07	62	62	1.0130E+02
14	14	1.4000E+07	63	63	6.1442E+01
15	15	1.3875E+07	64	64	3.7267E+01
16	16	1.3750E+07	65	65	2.2603E+01
17	17	1.3625E+07	66	66	1.3710E+01
18	18	1.3500E+07	67	67	8.3153E+00
19	19	1.3375E+07	68	68	5.0435E+00
20	20	1.3250E+07	69	69	3.0590E+00
21	21	1.3125E+07	70	70	2.3824E+00
22	22	1.3000E+07	71	71	1.8554E+00
23	23	1.2750E+07	72	72	1.4450E+00
24	24	1.2500E+07	73	73	1.1254E+00
25	25	1.2250E+07	74	74	8.7642E-01
26	26	1.2000E+07	75	75	6.8256E-01
27	27	1.1750E+07	76	76	5.3158E-01
28	28	1.1500E+07	77	77	4.1399E-01
29	29	1.1250E+07	78	78	3.8000E-01
30	30	1.1000E+07	79	79	3.6000E-01
31	31	1.0750E+07	80	80	3.3000E-01
32	32	1.0500E+07	81	81	3.1000E-01
33	33	1.0250E+07	82	82	3.0000E-01
34	34	1.0000E+07	83	83	2.9000E-01
35	35	7.7880E+06	84	84	2.8000E-01
36	36	6.0653E+06	85	85	2.6000E-01
37	37	4.7237E+06	86	86	2.4000E-01
38	38	3.6788E+06	87	87	2.2000E-01
39	39	2.8650E+06	88	88	1.8000E-01
40	40	2.2313E+06	89	89	1.6000E-01
41	41	1.7377E+06	90	90	1.4000E-01
42	42	1.3534E+06	91	91	1.0000E-01
43	43	1.0540E+06	92	92	8.0000E-02
44	44	8.2085E+05	93	93	6.0000E-02
45	45	4.9787E+05	94	94	4.0000E-02
46	46	3.0197E+05	95	95	2.5300E-02
47	47	1.8316E+05	96	96	1.5000E-02
48	48	1.1109E+05	97	97	7.0000E-03
49	49	6.7379E+04	98	98	4.0000E-03

TABLE 12. COMPARISON OF ANISN (EG&G) AND RAFFLE NEUTRON ABSORPTION AND LEAKAGE RATES IN STARFIRE

(absorptions/cm^3-sec per fusion neutron)

Region	ANISN (EG&G) 100-Group DLC37	ANISN(EG&G) 35-Group Flung	94-Gp RAFFLE	99-Gp RAFFLE
First Wall	0.1317	0.1456	0.1255 ± .0034[a]	0.1283 ± .0020[b]
Multiplier	0.0546	0.0540	0.0511 ± .0008	0.0512 ± .0005
Second Wall	0.0455	0.0507	0.0434 ± .0009	0.0435 ± .0005
Blanket	1.2549	1.2264	1.2504 ± .0091	0.2474 ± .0046
Reflector	0.0100	0.0172	0.0097 ± .0007	0.0093 ± .0003
Total Absorption	1.4967	1.4939	1.4801 ± .0098	1.4797 ± .0050
Neutron Leakage from Reflector	0.0470	0.0442	0.0556	0.0540
Total Neutron Loss	1.544	1.538	1.536	1.534

(a) 2σ uncertainties resulting from 31000 histories.

(b) 2σ uncertainties resulting from 105000 histories.

TABLE 13. TRITIUM BREEDING RATIO FOR STARFIRE BLANKET

Reaction	ANISN(EG&G) DLC37F[a] DLC37F[b] 100 Groups	ANISN(EG&G) DLC37F MACKLIB IV 100 Groups	ANISN(EG&G) FLUNG MACKLIB IV 35 Groups	ANSIN(ANL) VITIMIN C VITAMIN C 46 Groups	RAFFLE ENDF/B V ENDF/B v 94 Groups	RAFFLE ENDF/B V ENDF/B V 99 Groups
$^{6}Li(n,\alpha)T$	1.060	1.065	1.042	1.142	1.070 ± .006[c]	1.067 ± .005
$^{7}Li(n,n'\alpha)T$	0.076	0.076	0.079	0.079	0.080 ± .001	0.081 ± .001
Total	1.136	1.141	1.121	1.217	1.150 ± .006	1.148 ± .005

(a) Data set used to compute flux.

(b) Data set used to compute TBR.

(c) 2σ uncertainties.

TABLE 14. REACTION RATES FOR TMHR

Reaction	TRW TARTNP 171 Groups ENDF/B V ENDF/B V	EG&G RAFFLE 94 Groups ENDF/B V ENDF/B V	EG&G ANISN 100 Groups DLC37 MACKLIBIV	GA ANISN 25 Groups DLC37 MACKLIB	EG&G ANISN 25 Groups VITAMIN C MACKLIB	EG&G ANISN 35 Group FLUNG MACKLIBIV
$^{6}Li(n,T)$	0.85	0.917 ± .0054[(a)]	0.90	0.95	1.06	0.90
$^{7}Li(n,n'T)$	0.0034	0.00376 ± .00004	0.0036	0.0037	0.0037	0.0037
Be(n,T)	0.019	0.2160 ± .00019		0.020	0.029	
Th(n,f)	0.0014	0.00158 ± .00002	0.0015	0.0015	0.0015	
Th(n,2n)	0.0039	0.00440 ± .00009		0.0045	0.0047	
Th(n,3n)	0.0006	0.00083 ± .00002		0.0006	0.0007	
Th(n,γ)	0.44		0.524	0.51	0.50	
Fe(n,2n)	0.048	0.0515 ± .0004		0.050	0.050	
Fe(n,p)	0.020	0.202 ± .0002		0.020	0.020	
Fe(n,α)	0.0055	0.057 ± .0000 .0001		0.011	0.0057	
Be(n,2n)	1.36	1.5460 ± .0142		1.50	1.50	
Be(n,α)	0.14	0.1537 ± .0019		0.15	0.16	

(a) 2σ uncertainties resulting from 56000 histories. Half of these were fission neutron daughters produced by fusion neutrons.

APPENDIX A

EFFECT OF THERMAL NEUTRON CROSS SECTION WEIGHTING ON STARFIRE TRITIUM BREEDING RATIO

A1-INTRODUCTION

Neutronics calculations to predict tritium breeding and heating rates in fusion reactor blankets commonly rely on multigroup cross section libraries that employ only one group covering the thermal neutron energy range. To obtain thermal group cross sections, the energy dependent pointwise data from ENDF/B files are typically weighted with an assumed Maxwellian flux distribution. For example, the widely used 121-group DLC37 library[1] developed at ORNL assumes an 800K Maxwellian below 0.414 eV. Many cross section sets in use are collapsed from the 207-group VITAMIN C library[2] using various assumed weighting functions. VITAMIN C, which was developed specifically for the fusion reactor community, assumes a 1/E flux dependence from 0.414 eV to 0.125 eV and a 300K Maxwellian distribution below 0.125 eV. For most fusion blanket designs, spectrum hardening by lithium absorption will result in a thermal neutron energy spectrum that departs significantly from a Maxwellian shape. The inappropriate weighting spectrum will result in incorrect thermal group cross sections and reaction rates.

To determine the error in the STARFIRE tritium breeding ratio (TBR) due to using DLC37 or VITAMIN C weighting, the thermal neutron space-energy distribution in STARFIRE[3] is first computed with 39-group transport theory using the SCAMP code[a]. Ten of these groups fall below 0.414 eV. The multithermal group solution from SCAMP is then used to collapse cross sections to one thermal group which are then used in ANISN[5] along with EPR fast-groups data to compute the tritium breeding. The SCAMP calculations and results are described in Section A2. Also shown in Section A 2 is a comparison of the STARFIRE blanket spectrum with Maxwellian spectra and a spectrum computed for an infinite medium of blanket material. The infinite-medium spectrum is computed with a B-1 approximation using the INCITE[6] program. The TBR results of ANISN calculations made with appropriately averaged thermal group cross sections from SCAMP are discussed in Section A3.

(a) SCAMP is a multigroup version of the TOPIC code[4].

A2-CALCULATION OF THERMAL NEUTRON SPECTRUM IN THE STARFIRE BLANKET

A2.1 SCAMP Model

The space-dependent thermal neutron energy spectrum for STARFIRE was computed with SCAMP using cylindrical geometry and an S_6 angular quadrature. The spatial model is shown in Table A-1. The energy structure of the 39-group library is given in Table A-2. The library contains only P_0 and P_1 scattering cross sections. Scattering kernels were not available for lithium so that thermal neutron scattering with lithium was assumed to result in no energy change. However, since the lithium scattering cross section is only 1 barn, lithium scattering is small compared to the 3.8-b scattering cross section of oxygen (in $LiAlO_2$) and the 20-b cross section of water. Therefore, thermal neutron energy transfer by lithium scattering can be neglected.

A unit isotropic source is used in group 1. Note that the library does not extend to DT fusion neutron energies, thus, the source energy averages about 8 MeV. As a result, SCAMP could not be used directly to compute tritium breeding for STARFIRE. (The P1 scattering approximation would also make the results questionable.) However, the thermal neutron spectrum is insensitive to whether the slowing down source into the thermal energy range originated from 14-MeV neutrons or 8-MeV neutrons.

A2.2 Comparison of Maxwellian Spectra with Computed Blanket Spectra

SCAMP results show that the thermal neutron energy spectrum varies considerably across the blanket. In (and near) the multiplier and reflector regions, the spectrum is much softer than it is in the highly absorbing blanket region. This result is shown in Figure A-1. Note from the figure that near the second wall the spectrum is quite soft and resembles a Maxwellian, due to leakage into the blanket of neutrons thermalized in the less absorbing second wall and multiplier regions. In the center of the blanket, the only thermal neutrons present come from fast neutrons slowing down in the immediate vicinity. In this case, the ^6Li absorption hardens the spectrum so much that it looks nothing like a Maxwellian at 800K.

Since leakage effects are gone a few centimeters away from the second wall and reflector boundaries, the thermal spectrum rapidly approaches the shape it would have in an infinite medium. This is shown in Figure A-2 where the SCAMP flux in the central 10 cm of the blanket is compared with an infinite medium spectrum (Buckling = 0.0) computed with INCITE using a B-1 approximation. In Figure A-3, the INCITE spectrum is compared with Maxwellian distributions for three temperatures. The spatially averaged spectrum (flux-volume weighted) for the STARFIRE blanket is compared in Figure A-4 with the 800K Maxwellian spectrum assumed for EPR library generation. The computed spectrum is seen to be much harder than the assumed Maxwellian shape.

A3-TBR RESULTS WITH SCAMP COLLAPSED THERMAL CROSS SECTIONS

The ^{6}Li 10-group thermal (0-0.414 eV) microscopic absorption cross sections used in SCAMP are given in Table A-3. Weighting these cross sections by the SCAMP thermal flux spectrum shown in Figure A-4 results in an average ^{6}Li thermal cross section of 438.8b. This compares with the 507b and 750b cross sections assumed in the DLC37 and FLUNG libraries, respectively. Only at the edges of the blanket by the second wall and the reflector where the spectrum is softest does the cross section exceed 500b. It is 549b at the interface with the second wall and 522b at the reflector interface. Within a few centimeters of either boundary, the spectrum averaged cross section drops to about 340b.

The TBR error caused by inappropriate thermal group cross sections was determined with ANISN calculations in which all thermal group cross sections for all regions were changed to agree with SCAMP collapsed values. Compared to the case with all DLC37 data, the SCAMP collapsed thermal-group data lowered the ^{6}Li thermal neutron absorption rate by 10% due primarily to decreased thermal neutron leakage into the blanket from the second wall region. The smaller leakage is caused by a softer spectrum (and hence higher thermal neutron absorption) in the multiplier and second wall regions than the 800K Maxwellian assumed in DLC37F. Lithium-6 thermal neutron capture contributes only 12-13% to the total TBR. Therefore, the 10% error in thermal neutron capture rates in the blanket results in a 1.3% error in the STARFIRE TBR.

Changing only the ^{6}Li cross section has very little effect on the TBR. This was shown by an ANISN calculation in which the ^{6}Li total cross section was changed to reflect the 750-barn absorption cross section used in FLUNG. Compared to the case with all DLC37 data, there was practically no effect in TBR. The thermal flux in the blanket region was simply reduced by an amount that compensates for the cross section increase.

The 1.3% error in TBR for STARFIRE due to using a single thermal group with inappropriate cross sections is significant but not serious. However,

the error will be design dependent and could be serious for other blanket designs if they were more heterogeneous or more thermalized than STARFIRE. For example, additional water coolant in a design like STARFIRE would increase the error. A heterogeneous design that attempted to alternate layers of moderator material (coolant or multiplier) with breeding material could be susceptible to large errors. On the other hand, liquid-lithium blanket designs have very hard flux spectra so that thermal neutrons reaction rates are very small and errors in thermal neutron cross sections would be insignificant.

A4 REFERENCES

1. D. M. Plaster, R. T. Santoro, W. E. Ford, III, Coupled 100-Group Neutron and 21-Group Gamma-Ray Cross Sections for EPR Calculations, DLC-37, ORNL-TM-4812, April 1975, updated to DLC-37F, October 1979.

2. R. W. Roussin, et.al., VITAMIN-C: The CTR Processed Multigroup Cross Section Library for Neutronics Studies, ORNL/RSIC-37, 1980; also available as DLC-41.

3. STARFIRE - A Commercial Tokamak Fusion Power Plant Study, Argonne National Laboratory Report, ANL/FPP-80-1, September 1980.

4. G. E. Putnam, TOPIC - A FORTRAN Program for Calculating Transport of Particles in Cylinders, IDO-16968, April 1964.

5. W. W. Engle, jr., A User's Manual for ANISN, A One-Dimensional Discrete Ordinates Transport Code with Anisotropic Scattering, K-1693, Computing Technology Center, 1967.

6. R. L. Curtis and R. A. Grimesey, INCITE--A FORTRAN-IV Program to Generate Thermal Neutron Spectra and Multi-group Constants Using Arbitrary Scattering Kernels, IN-1062, November 1967.

TABLE A-1. SCAMP STARFIRE MODEL

Region	Material	Outer Radius (cm)	Mesh Spacing (cm)
1	Void-Source	150.0	10.0
2	Void	200.0	10.0
3	First Wall	201.0	0.1
4	Be Multiplier	206.0	0.33333
5	Second Wall	207.0	0.1
6	Blanket	210.0	0.0625
7	Blanket	217.0	0.14
8	Blanket	227.0	0.5
9	Blanket	234.0	0.25
10	Blanket	237.0	0.0625
11	Reflector	252.0	0.5
12	Shield	257.0	0.25

TABLE A-2. SCAMP LIBRARY GROUP STRUCTURE

Group	Upper Energy (eV)
1	10.00 + 6
2	6.07 + 6
3	3.60 +6
4	7.14 + 6
5	8.21 + 5
6	3.88 + 5
7	1.83 + 5
8	8.65 + 4
9	4.09 + 4
10	1.93 + 4
11	9.12 + 3
12	4.31 + 3
13	2.04 + 3
14	9.61 + 2
15	5.83 + 2
16	3.54 + 2
17	2.15 + 2
18	1.30 + 2
19	78.9
20	47.9
21	29.0
22	17.6
23	10.68
24	6.48
25	3.93
26	2.38
27	1.445
28	0.876
29	0.532
30	0.414
31	0.31
32	0.24
33	0.18
34	0.14
35	0.10
36	0.06
37	0.0253
38	0.015
39	0.004

TABLE A-3. ^{6}Li THERMAL NEUTRON ABSORPTION CROSS SECTIONS

Group	σ (barns)
30	250.11
31	286.82
32	329.58
33	377.73
34	439.16
35	539.50
36	744.89
37	1058.10
38	1531.50
39	3046.26

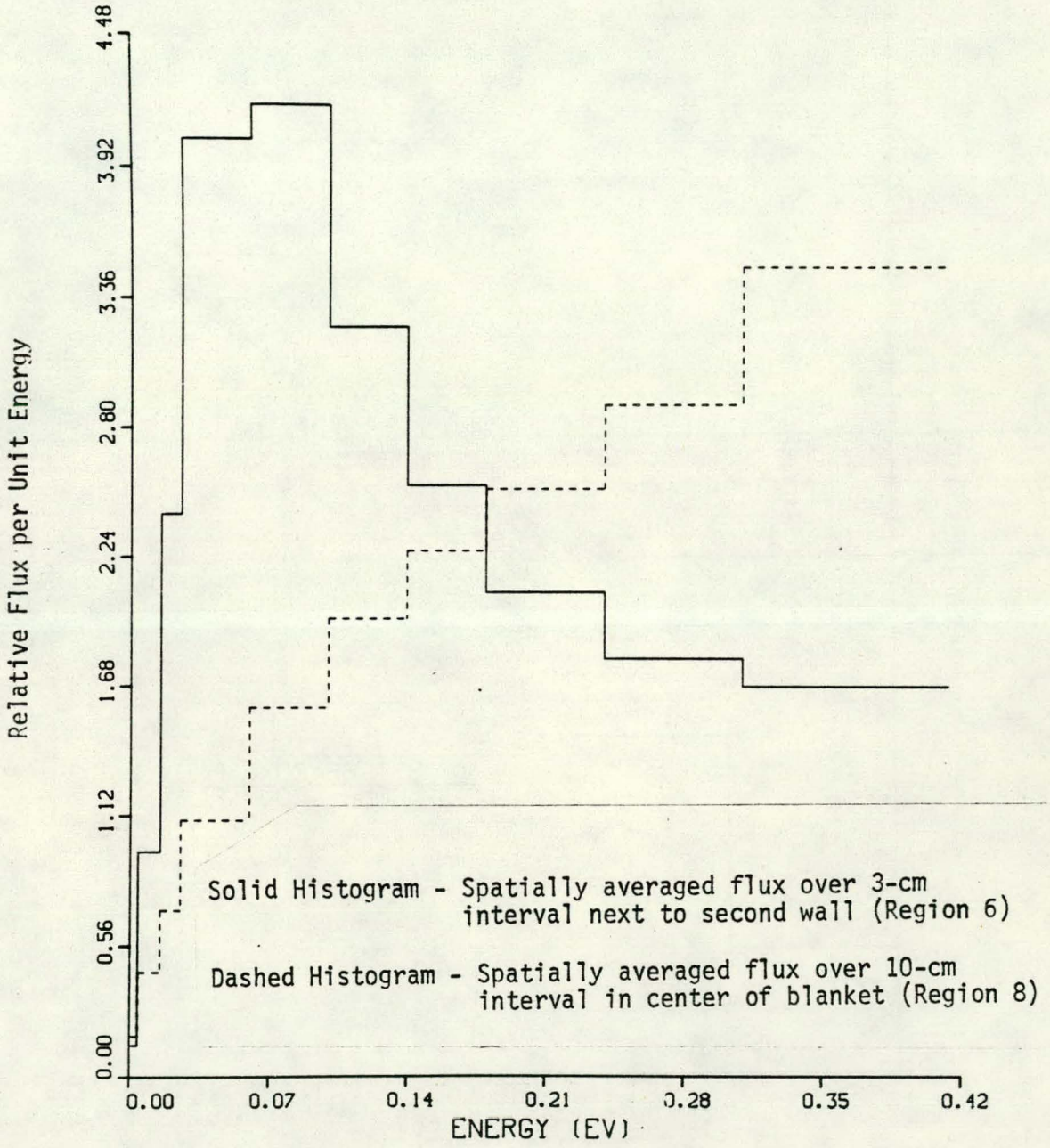

Figure A-1. Spatial Variation of Thermal Spectrum in Blanket

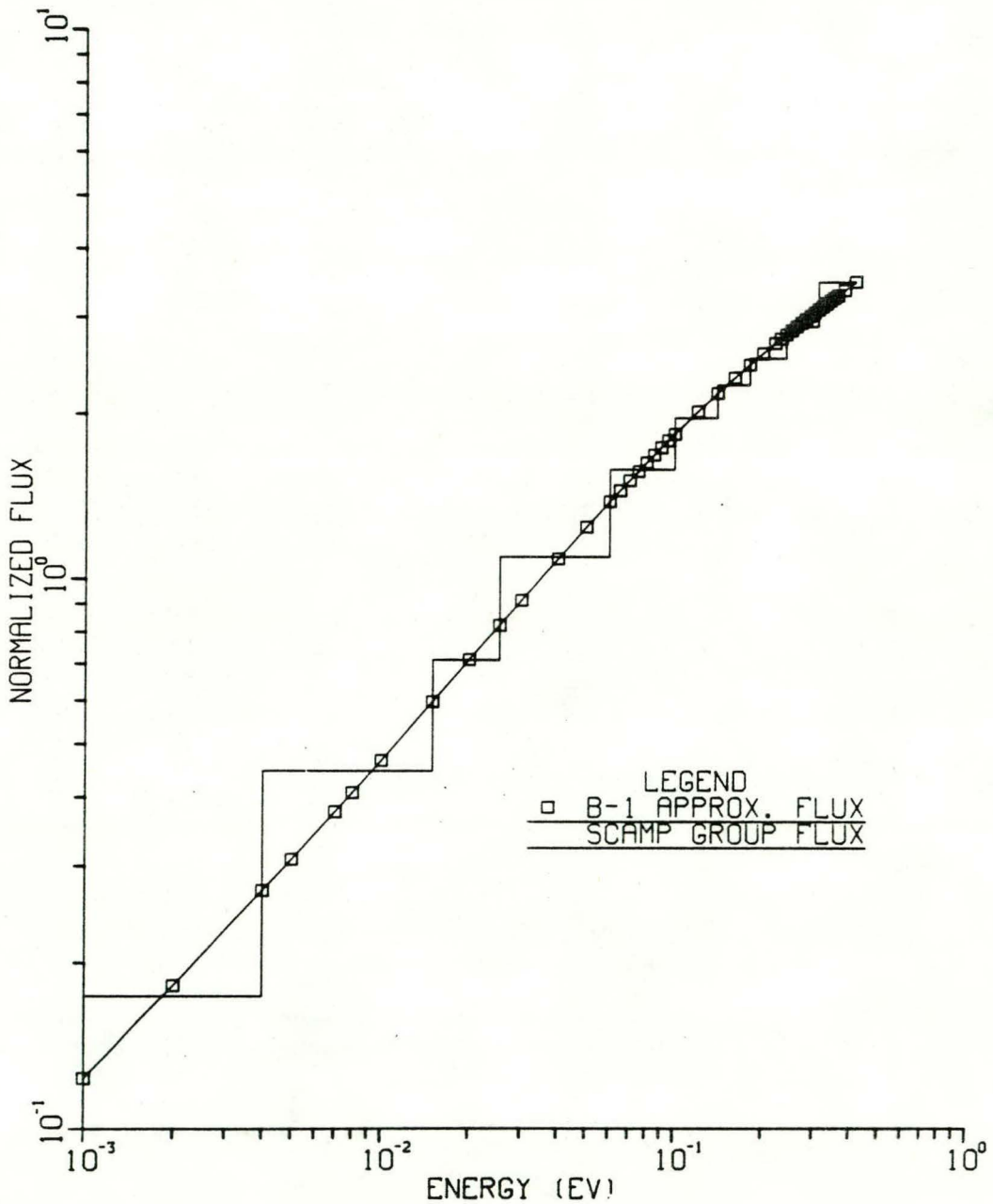

Figure A-2. Comparison of Thermal Spectrum in Central 10 cm of STARFIRE Blanket with Infinite Medium Spectrum.

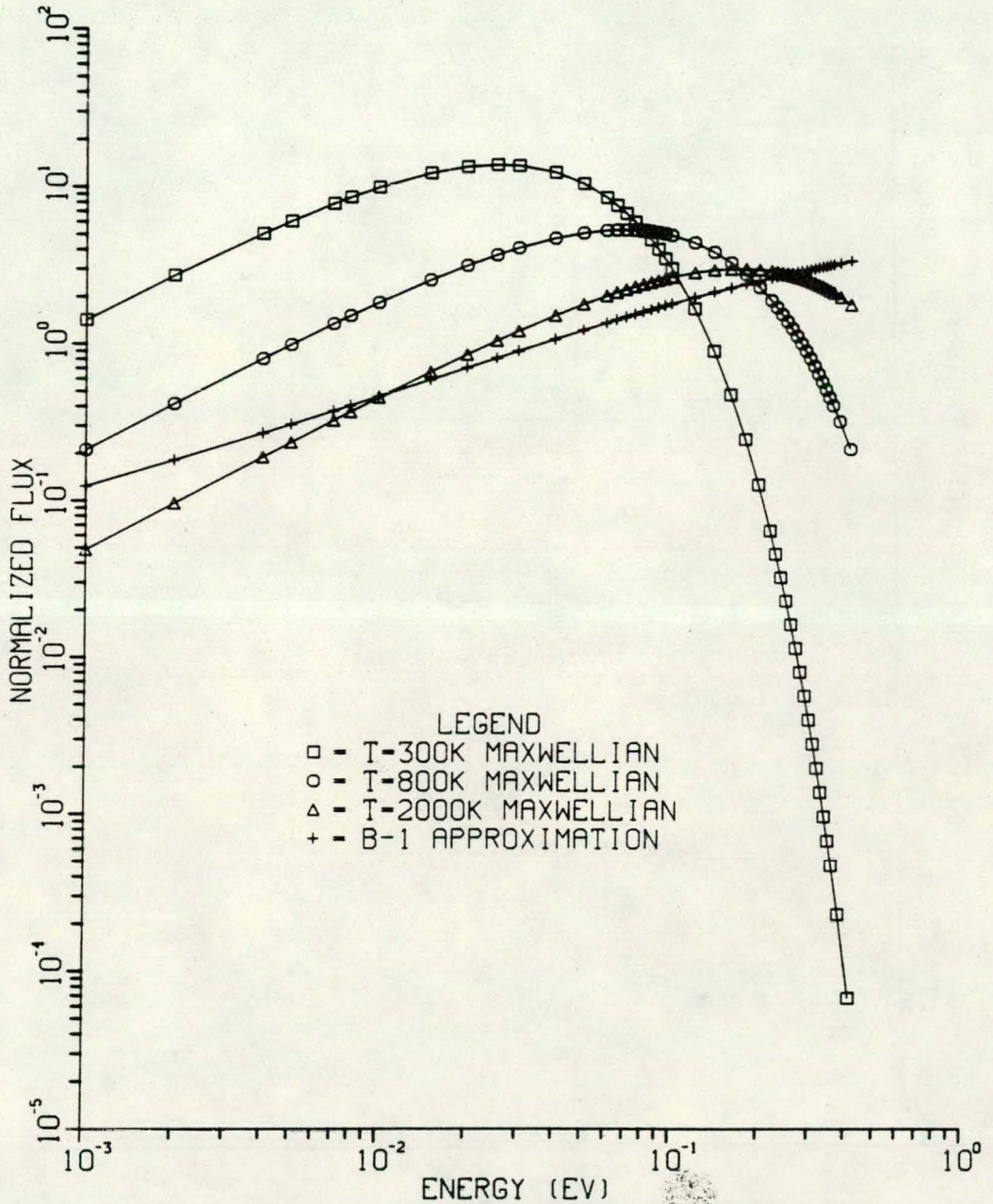

Figure A-3. Comparison of Maxwellian Spectra with Infinite Medium Spectrum from B-1 Approximation.

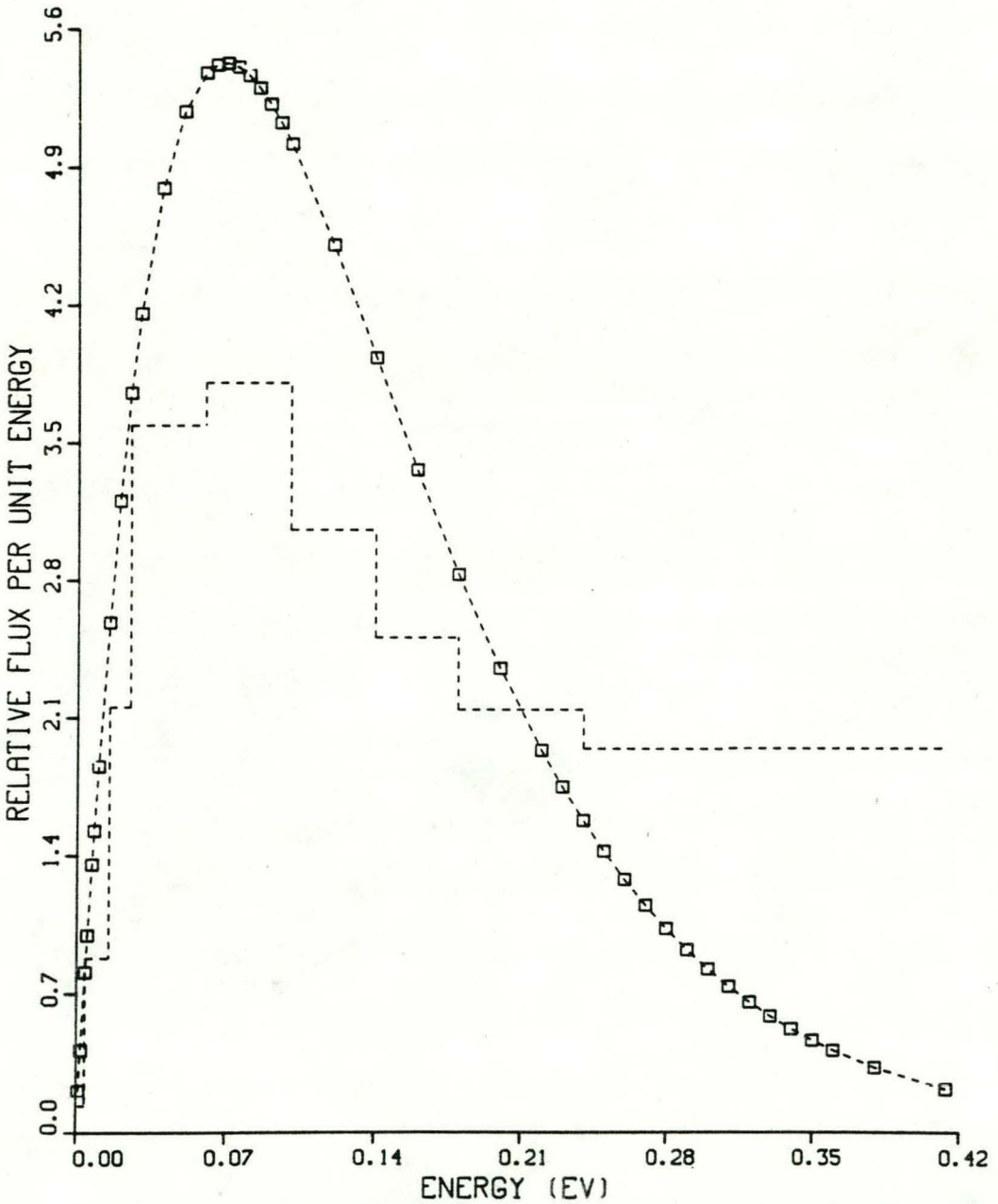

Figure A-4. Comparison of Spatially Averaged Spectrum for STARFIRE Blanket with 800K Maxwellian Spectrum.

APPENDIX B

CONFIGURATION CONTROL NUMBERS FOR CODES AND DATA

For retrieval purposes and a permanent record of the calculations, the codes and data sets used in this study are filed under the following EG&G configuration control numbers.

Item	File Numbers
RAFFLE	F00555
94-Group RAFFLE LIBRARY	F00576
99-Group RAFFLE LIBRARY	F00576
ANISNAB	H0048885
DLC37F	H001885B
FLUNG	F00577
MACKLIBIV	F005555
HEATLZB (Collapsed MACKLIBIV)	F00555
ACTIVE5 (Computes Reaction Rates)	F00555
SCAMP	F00128
INCITE LIB.	F00630
HEATLBB	F00631